Thin Solid Films xxx (xxxx) xxx–xxx

Contents lists available at ScienceDirect

Thin Solid Films

journal homepage: www.elsevier.com/locate/tsf

Proton beam flux dependent work function of mono-layer MoS_2

Sangwoo Kwon[a], Soo Ho Choi[a], You Joong Kim[a], Im Taek Yoon[b], Woochul Yang[a,*]

[a] Department of Physics, Dongguk University, Seoul 04620, Republic of Korea
[b] Quantum Functional Semiconductor Research Center, Dongguk University, Seoul 04620, Republic of Korea

ARTICLE INFO

Keywords:
Monolayer
Molybdenum disulfide
Proton irradiation
Work function
Defect formation
Sulfur-vacancy

ABSTRACT

Monolayer (ML)-molybdenum disulfide (MoS_2) with a direct band gap of ~1.8 eV exhibits considerable potential for advanced electronic and optical device applications. The surface electronic properties of ML-MoS_2 need to be controlled for developing novel MoS_2-based devices. In this study, we investigated the work function variation of chemical vapor deposition-grown ML-MoS_2 that was controlled by proton irradiation. The crystallinity of the ML-MoS_2 was confirmed by micro-Raman and Photoluminescence measurements. The work functions of the ML-MoS_2 irradiated with varying proton beam flux were measured by Kelvin probe force microscopy. As the ML-MoS_2 were exposed to the proton beam flux ranging from 1×10^{12} to 1×10^{14} protons/cm^2 at the same beam energy of 10 MeV, the contact potential difference of the MoS_2 increased up to about 0.108 V with increased proton beam flux. Based on the referenced value of the Au work function (≈5.1 eV), the work functions of non-treated ML-MoS_2 and proton-irradiated ML-MoS_2 with a proton beam flux of 1×10^{14} protons/cm^2 were determined to be 5.031 eV and 4.992 eV, respectively. The decrease of the work function of the MoS_2 with increased proton beam flux is due to the defect formation induced by proton irradiation. We suggest the possibility of engineering the surface potential and electronic properties of ML-MoS_2 through controlling proton irradiation conditions.

1. Introduction

Two-dimensional (2D) transition metal dichalcogenides (TMDCs), which are semiconductors of the MX_2 type (M: a transition metal atom, X: a chalcogen atom) [1,2], are layered materials that area widely studied for harvesting fundamental science and emergent applications in nanoelectronics and optoelectronics. Molybdenum disulfide (MoS_2) is a prototypical TMDC material [3]. Monolayer MoS_2 (ML-MoS_2) is composed of three-atomic-thick S-Mo-S stacks. Unlike ML-MoS_2 with a direct bandgap (≈1.8 eV), the bulk MoS_2 has an indirect bandgap of ~1.23 eV [4]. Moreover, chemical vapor deposition (CVD) methods for the large-area growth of ML-MoS_2 have recently been optimized [5,6].

The variation of the electrical properties in MoS_2 has already been studied for the layer number of MoS_2. However, focus needs to be placed on engineering the material properties in ML-MoS_2 through external treatments. One of the many methods used for changing the electrical property of 2D materials is to control defect-sites [7]. For example, M. R. Islam et al. [8] demonstrated that the electrical property of ML-MoS_2 can be significantly tuned from the semiconducting to the insulating regime via defect engineering by oxygen plasma. ML-MoS_2 has two types of atomic defects: sulfur (S)-vacancy and molybdenum (Mo)-vacancy. The formation energy of S-vacancy is lower than that of Mo-vacancy. Thus, S vacancies are energetically more favorable than Mo vacancies [9]. The intrinsic defects can be produced unintentionally in mechanically exfoliated or CVD-grown MoS_2. However, it is not a repetitive phenomenon. We therefore focused on employing the proton beam irradiated with the high proton energy to intentionally produce atomic-defects in ML-MoS_2. Several experimental studies have been carried out on the characterization of 2D materials related to the defects produced by proton beam irradiation. For instance, S. Mathew et al. [10] studied the effect of proton beam irradiation on the layer number of graphenes and substrates. They also reported that proton-irradiated MoS_2 exhibited ferrimagnetic behavior [11]. While the electrical properties of field effect transistor devices based on proton-irradiated multilayer MoS_2 were investigated by Kim et al. [12]. However, no fundamental studies have been carried out on the variation of the surface potential in proton-irradiated ML-MoS_2. This study focused on the correlation of the surface potential of ML-MoS_2 with defective-sites produced by proton ions.

In this study, we prepared ML-MoS_2 samples exposed to various proton beam fluxes and measured the variation in work function by Kelvin probe force microscopy (KPFM) to analyze the modification of electronic properties related to the defective-sites on ML-MoS_2. We discuss the electronic band structure of ML-MoS_2 before and after

* Corresponding author.
E-mail address: wyang@dongguk.edu (W. Yang).

https://doi.org/10.1016/j.tsf.2018.03.078
Received 29 November 2017; Received in revised form 24 February 2018; Accepted 28 March 2018

proton irradiation with a varying proton flux. We confirmed that the results of the KPFM measurements are consistent with those obtained from the first-principles (density functional theory) calculation.

2. Experiment details

ML-MoS_2 was grown in a CVD furnace with a 2 in. quartz tube including zone 1 and zone 2 of the furnace. Zone 1 was used for evaporation of S powder and zone 2 was used for evaporation of the Mo precursor and growth of MoS_2 on the substrate. The distance between zone 1 and zone 2 is 35 cm. The Si substrate with 300 nm thick SiO_2 was prepared by treatment with piranha solution (H_2SO_4:H_2O_2 = 3:1) for converting hydrophobic surface to hydrophilic surface. Mo precursor (ammonium molybdate tetrahydrate solution, $(NH_4)_6Mo_7O_{24}$•4(H_2O)) of 4 ml was coated on the substrate via spin-coating. The substrate was then placed in the center of zone 2 while S powder was loaded on the center of zone 1. Prior to growth, the system was purged using high purity argon gas (99.999%) at 500 sccm for 10 min to remove residual gases. The temperatures of zone 1 and zone 2 were elevated from room temperature to 350 °C and 800 °C for 15 min, respectively. During growth, the temperature was maintained for 10 min. After growth, the furnace was rapidly cooled to room temperature. An argon flow rate of 500 sccm at atmospheric pressure was maintained throughout the entire growth process. Fig. 1(a) shows that the MoS_2 flakes are well-grown on the SiO_2/Si substrate. First, to confirm that the as-grown MoS_2 flakes are a monolayer structure, optical microscopy (Nikon LV-IM, Nikon) and micro-Raman and photoluminescence (PL) spectroscopy (XperRAM100, Nanobase Inc., Korea) were used with a 532 nm laser excitation (average power of < 0.5 mW; exposure time of 1 s) at room temperature in ambient condition. After the characterization of the ML-MoS_2, the flakes were transferred onto the Au substrate by conventional transfer method. Considering the proton beam spot size (~10 mm), the $5 \times 5\ mm^2$ sized ML-MoS_2 was transferred onto the center of the $1 \times 1\ cm^2$ Au substrate. The samples were then annealed at 350 °C under atmosphere for KPFM (N8-NEOS, BRUKER Inc., Germany) measurement.

The proton irradiation of the ML-MoS_2 samples was conducted on a proton beam line in a MC-50 cyclotron at the Korea Institute of Radiological and Medical Sciences (KIRAMS). The employed energy and current of the proton beam were fixed at 10 MeV and 10 nA, respectively. The proton irradiation times were 10, 101, and 1019 s, which correspond to the proton beam fluxes of 1×10^{12}, 1×10^{13}, and 1×10^{14} ions/cm^2 exposed to the ML-MoS_2/Au samples, respectively. The prepared samples are positioned at the center of the beam line and all of our experiments were carried out at room temperature.

The work function of the samples before and after proton beam irradiation was measured by using the KPFM technique. KPFM is an operating mode available in the atomic force microscopy (AFM) systems, and was used for measuring the variation in the local surface potential on the surface by employing a conducting AFM tip coated with Cr/Pt (Multi-75, Budgetsensors. Inc., Bulgaria). The measurement of the surface potential using KPFM is generally conducted by the interaction between the AFM tip and sample surface. In the KPFM measurement, the distinct work function between the sample and the substrate can be determined from the Contact Potential Difference (V_{cpd}). The contrast of local brightness in the KPFM image can be used to obtain V_{cpd}, which is defined as follows [13,14], $V_{cpd} = (\phi_{tip} - \phi_{sample}) / (-e)$ where ϕ_{tip} and ϕ_{sample} are the work functions of the AFM tip and the sample, respectively, and e is the electronic charge. When the tip and sample make contact with each other, the electrons move from the material with a low work function to that with a high work function until the Fermi levels of all materials are equal. The result voltage difference is referred to as V_{cpd}.

3. Results and discussion

The optical properties of CVD-grown MoS_2 were investigated by micro-Raman and PL spectroscopy as shown in Fig. 1. The optical microscopy image showed that high-quality MoS_2 flakes were grown on the SiO_2 substrate, as shown in Fig. 1 (a). The triangular shaped MoS_2 flake was selected for investigation of optical properties. Two typical Raman-active phonon modes of E^1_{2g} (centered at ~384 cm^{-1}) and A_{1g} (centered at ~403 cm^{-1}) were observed and the frequency spacing between the E^1_{2g} and A_{1g} peaks was about 19 cm^{-1}, as shown in Fig. 1(b). Our Raman results were consistent with the Raman results of ML-MoS_2 reported from other groups [15]. Also, the bandgap of the MoS_2 flake was determined to be ~1.86 eV through PL spectrum measurement (Fig. 1(c)), which indicates a monolayer MoS_2 [5,6]. It was thus confirmed that the CVD-grown MoS_2 flakes have a monolayer structure.

Before the AFM measurements, the number of protons irradiated on the few nano-sized areas of ML-MoS_2 was first quantitatively calculated. In the top view of ML-MoS_2 shown in Fig. 2, the distance between the two atoms (Mo or S) is about 3.122 Å [16]. The proton flux of 1×10^{14} protons/cm^2 on a substrate with $1 \times 1\ cm^2$ scale corresponds to the irradiation of a proton on the surface of the 3×3 unit cell (dashed line in Fig. 2) of ML-MoS_2, as shown in Fig. 2. After proton irradiation with a proton flux of 1×10^{12}, 1×10^{13} and 1×10^{14} protons/cm^2 on each ML-MoS_2/Au substrate sample, we conducted AFM measurements of the ML-MoS_2 flakes with similar shapes and sizes selected by optical microscopy. Considering the proton beam size (~1 cm), the entire surface ($5 \times 5\ mm^2$) of the ML-MoS_2 was affected by the protons.

Fig. 3 shows the AFM morphology and KPFM images of the ML-MoS_2/Au samples before and after proton beam irradiation with proton flux of 1×10^{12}, 1×10^{13}, and 1×10^{14} protons/cm^2. For all morphologies of the samples (Fig. 3(a)–(d)), the ML-MoS_2 are easily distinguished from the Au substrate. The region of the relatively flat surface exhibits the ML-MoS_2 while the region of the rough surface indicates the Au substrate. After transferring ML-MoS_2 flakes onto the Au substrate, an annealing process was performed to stabilize the

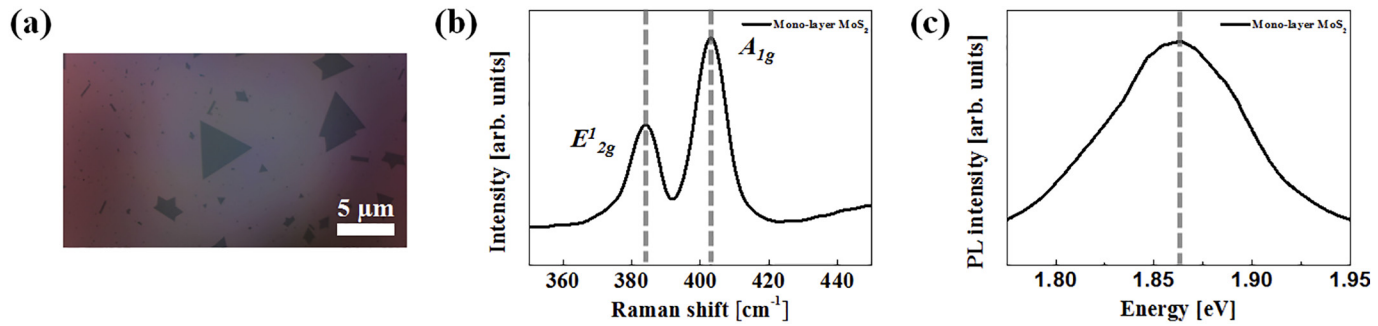

Fig. 1. (a) Optical microscopy image of ML-MoS_2: high-quality ML-MoS2 flakes are grown on the SiO_2/Si substrate. (b) Micro-Raman of ML-MoS_2: E^1_{2g} and A_{1g} peaks are centered at 384.0 cm^{-1} and 402.8 cm^{-1}, respectively. (c) PL spectrum of ML-MoS_2: the bandgap of ML-MoS2 is 1.86 eV.